1992

A Study of the Leakage Performance for the Plain Seal with Injection

K. S. Lee
Hanyang University

W. S. Kim
Hanyang University

K. Y. Kim
Hanyang University

C. H. Kim
Korea Institute of Science and Technology; Korea

A Study of the Leakage Performance for the Plain Seal with Injection

Kwan Soo Lee[1], Woo Seung Kim[2], Ki Yeon Kim[3], Chang Ho Kim[4]

[1] Professor, Hanyang University, Seoul, Korea
[2]Assistant professor, Hanyang University, Seoul, Korea
[3] Graduate Research Assistant, Hanyang University, Seoul, Korea
[4] Senior Research Scientist, Korea Institute of Science and Technology, Seoul, Korea

ABSTRACT

A numerical analysis is performed on the turbulent flow in the plain seal with injection. The effects of parameters such as rotation speed, injection speed, clearance ratio, injection angle, and axial injection location on flow pattern and leakage performance are investigated. SIMPLER algorithm is used to solve the governing Navier-Stokes equation for steady, incompressible turbulent flow with the k-ε turbulence model. It is found that the leakage performance is significantly enhanced with injection. The increasing the injection flow rate and rotation speed of the shaft increases the leakage performance. At the injection angle of 90 degree, the leakage coefficient becomes minimum. The pressure drop is a maximum at axial center location but injection location has little effect on the pressure drop. Clearance ratio has a substantial effect on the pressure drop.

NOMENCLATURE

b : length from inlet to injection location
c : clearance
c_1, c_2, c_μ : turbulence model constants
d : injection width
G : turbulence source term
k : turbulence kinetic energy
K : dimensionless turbulence kinetic energy
L : total axial length of seal
p : pressure
P : dimensionless pressure
Re : Reynolds number
r_i : radius of rotor
r_o : radius of stator
u,v,w : time-averaged velocities
U,V,W : dimensionless velocities
x,r : coordinates
X,R : dimensionless coordinates
α : inflow angle of injection
ε : dissipation rate of turbulence kinetic energy
σ_k : Prandtl constant of turbulence kinetic energy
σ_ε : Prandtl constant of turbulence kinetic energy dissipation rate
ν : dynamic viscosity
τ : shear stress
ρ : density
δ_{ij} : kronecker delta — 1 if i = j; 0 if i ≠ j
κ : von Karman constant
θ : circumferential coordinate

Superscript
′ : fluctuating component of velocity
+ : dimensionless variable at the wall
* : dimensionless variable

Subscript
in : inflow of fluid
w : wall

1. INTRODUCTION

Seals are used to reduce fluid leakage due to the pressure gradient in fluid machinery such as turbines, compressors and pumps. In general, seal may be classified as follows : contacting seals and noncontacting seals. The contacting seal cannot be used due to the metallurgical limitations to sealing in locations where the temperature and/or the pressure are very high, and when the machine rotates at high speed. Therefore, the noncontact seal is usually used in fluid machines requiring high performance. The noncontact seal used in high-capacity fuel pump reduces the leakage between the stator and the impellers and affects the overall performance of the fuel pump. Seals need to be designed by considering that there must be a flow path accompanying active dissipation of the kinetic energy in region where the pressure gradient exists, and it has to be easy to manufacture them.

The labyrinth seal is difficult to manufacture because of the complexity of the configuration, and its life is not long, but it has superior leakage performance. Since the plain seal is relatively easy to manufature, the research has been recently directed towards improving the seal performance of plain seal by altering the design conditions. The problems considered thus far have been directed towads the dynamic behavior related to the seal-life and amount of leakage without describing the leakage phenomena. Nelson[1] studied two cases of the straight annular seal and tapered seal, and compared two cases for the rotor dynamic coefficients and amount of leakage. He employed a perturbation method to analyze the problem by using Hirs' turbulent bulk-flow model. Nordmann et al.[2] used the appropriate Navier-Stokes equation in connection with the k-ε model. By introducing a perturbation analysis in their differential equations, they obtained zeroth order equation for the center position and first order equation for small motions of the shaft about the center position. These equations are solved by a finite difference technique. The zeroth order equation describe the leakage flow while integrating the pressure solution of the first order equations yields the fluid forces and rotordynamic coefficients. As a result, this method can represent rotordynamic coefficient more accurately than previous one based on bulk flow theory. Childs et al.[3] designed various types of damper-seal in order to improve the dynamic behavior and leakage performance. They defined the leakage coeffieient which is a non-dimensional relative measure of the leakage to be expected from seals with the same radius. Stoff[4] investigated the incompressible flow in a labyrinth seal, in order to explain leakage phenomena against the mean pressure gradient by using the k-ε turbulence model. He experimentally verified the turbulence kinetic energy and turbulence dissipation rate for a comparison with the result of the turbulence model. Demko et al.[5] conducted a computational/experimental study on the incompressible flow in a labyrinth seal at low leakage rates over a wide range of seal rotation rates. Rhode and Sobolik[6] developed a new method for predicting the leakage through labyrinth seal and compared with measurements. They also examined the detailed cavity distribution of basic flow field quantities.

The objective of the present work is to numerically investigate the effects of various factors on leakage performance of the plain seal with injection. The factors considered in this study included the shaft rotation speed, injection inflow speed, clearance ratio, injection location and injection inflow angle.

2. MATHEMATICAL FORMULATION

2.1 Governing equations

The schematic diagram of the configuration considered is shown in Fig.1.

For the sake of simplicity it is assumed that the flow field is axisymmetric, steady, incompressible, two-dimensional turbulent flow, that the flow in circumferential direction is fully developed, and that the body force is negligible. The situation is governed by the time-averaged Navier-Stokes equation written in tensor notation.

$$\frac{\partial}{\partial x_j}(u_i u_j) = -\frac{1}{\rho}\frac{\partial P}{\partial x_j} + \frac{\partial}{\partial x_j}\left(\nu \frac{\partial u_i}{\partial x_j}\right) - \frac{\partial}{\partial x_j}\overline{(u_i' u_j')} \qquad (1)$$

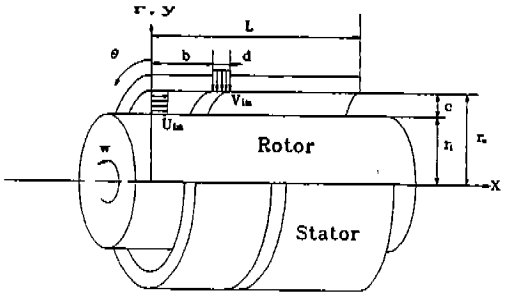

Fig.1 Schematic diagram of plain seal with injection

where $\overline{u_i' u_j'}$ is Reynolds stress which represents momentum transport by turbulent flow per unit mass. This term can be represented using Boussinesq's assumption.

$$-\overline{u_i' u_j'} = \nu_t \left(\frac{\partial u_i}{\partial x_j} + \frac{\partial u_j}{\partial x_i}\right) - \frac{2}{3}\delta_{ij} k \tag{2}$$

By developing transport equations for both k and ε , turbulent viscosity values can be calculated by the relation

$$\nu_t = \frac{c_\mu k^2}{\varepsilon} \tag{3}$$

The transport equations for the turbulent kinetic energy, k and the rate of dissipation of turbulent kinetic energy, ε are given by

$$\frac{Dk}{Dt} = \frac{\partial}{\partial x_j}\left(\frac{\mu_t}{\sigma_k}\frac{\partial k}{\partial x_j}\right) + \nu_t \left(\frac{\partial u_i}{\partial x_j} + \frac{\partial u_j}{\partial x_i}\right) - \varepsilon \tag{4}$$

$$\frac{D\varepsilon}{Dt} = \frac{\partial}{\partial x_j}\left(\frac{\mu_t}{\sigma_\varepsilon}\frac{\partial \varepsilon}{\partial x_j}\right) + c_1 \frac{\varepsilon}{k}\nu_t \left(\frac{\partial u_i}{\partial x_j} + \frac{\partial u_j}{\partial x_i}\right) - c_2 \frac{\varepsilon^2}{k} \tag{5}$$

The values of the turbulence constants chosen are presented in Table 1.

Table 1. Chosen values for turbulence constants

c_1	c_2	c_μ	σ_k	σ_ε
1.44	1.92	0.09	1.0	1.3

The standard k-ε turbulence model is applicable only to the flow regions at high turbulence Reynolds number and cannot be applied in near-wall region. Hence, the so-called wall-function approach is used in order to bridge the wall layer with the fully turbulent region.

Following dimensionless variables are introduced in the subsequent analysis.

$$x^* = \frac{x}{c}, \quad r^* = \frac{r}{c}, \quad U = \frac{u}{u_{in}}, \quad V = \frac{v}{u_{in}},$$

$$W = \frac{w}{u_{in}}, \quad K = \frac{k}{u_{in}^2}, \quad \varepsilon^* = \frac{\varepsilon}{u_{in}^2/c}, \quad P = \frac{p}{1/2\rho\, u_{in}^2},$$

$$\nu_t^* = \frac{\nu_t}{u_{in} c}, \quad Re = \frac{2 c u_{in}}{\nu} \tag{6}$$

With the introduction of the non-dimensional variables, the five governing equations for the present turbulent problem were found to all fit into a general elliptic equation form with the dependent variable denoted by ϕ.

This general equation form is

$$\frac{\partial}{\partial x_j}(U_j\phi) = \frac{\partial}{\partial x_j}\left(\Gamma_\phi \frac{\partial \phi}{\partial x_j}\right) + S_\phi \tag{7}$$

where ϕ represents any of the dependent variables, and the corresponding values of Γ_ϕ and S_ϕ are listed in Table 2.

Table 2. The form of the diffusion coefficient and source term in the general equation for ϕ

ϕ	Γ_ϕ	S_ϕ
U	$\frac{2}{Re}+\nu_t^*$	$\frac{\partial}{\partial X}(\nu_t^*\frac{\partial U}{\partial X}) + \frac{1}{R}\frac{\partial}{\partial R}(\nu_t^* R\frac{\partial V}{\partial X}) - \frac{1}{\rho}\frac{\partial P}{\partial X}$
V	$\frac{2}{Re}+\nu_t^*$	$\frac{W^2}{R} - \nu_e^*\frac{V}{R^2} - \nu_t^*\frac{V}{R^2} + \frac{\partial}{\partial X}(\nu_t^*\frac{\partial U}{\partial R}) + \frac{1}{R}\frac{\partial}{\partial R}(\nu_t^* R\frac{\partial V}{\partial R}) - \frac{1}{\rho}\frac{\partial P}{\partial R}$
W	$\frac{2}{Re}+\nu_t^*$	$-\frac{VW}{R} - \nu_e^*\frac{W}{R^2} - \frac{W}{R}\frac{\partial \nu_t^*}{\partial R}$
K	ν_t^*/σ_k	$G - \varepsilon^*$
ε^*	$\nu_t^*/\sigma_\varepsilon$	$(c_1 G\varepsilon^* - c_2\varepsilon^{*2})/K$

Here, G is given by

$$G = \nu_t^*\left[2\left(\left(\frac{\partial U}{\partial X}\right)^2+\left(\frac{\partial V}{\partial R}\right)^2+\left(\frac{V}{R}\right)^2\right) + \left(\frac{\partial U}{\partial R}+\frac{\partial V}{\partial X}\right)^2 + \left(R\frac{\partial}{\partial R}\left(\frac{W}{R}\right)\right)^2 + \left(\frac{\partial W}{\partial X}\right)^2\right]$$

2.2 Boundary conditions

The boundary conditions are taken as ;

At inlet;

$$u = u_{in},\ v = 0,\ w = 0$$
$$\text{with}\quad k = 0.005\,u_{in}^2,\quad \varepsilon = 0.1\,k^2 \tag{8}$$

At outlet;

$$\frac{\partial v}{\partial x} = \frac{\partial w}{\partial x} = \frac{\partial k}{\partial x} = \frac{\partial \varepsilon}{\partial x} = 0 \tag{9}$$

At inner wall;

$$u = 0,\ v = 0,\ w = w_i$$
$$k = 0,\ \varepsilon = 0 \tag{10}$$

At the injection location of the outer wall;

$$u = v_{in}\cos\alpha,\ v = v_{in}\sin\alpha,\ w = 0$$
$$\text{with}\quad k = 0.005\,v_{in}^2,\quad \varepsilon = 0.1\,k^2 \tag{11}$$

2.3 Numerical computation and verification

Since the governing equations fit into a common form, it is desirable to obtain a solution technique that solves equations of the general form given by equation (7). The equation (7) is discretized using a finite-difference scheme and the resulting discretized equations are solved iteratively using the SIMPLER algorithm as outlined in ref.[9].

Grid dependence tests were performed in order to determine the grid size effect. The tests show that 60×22 control volume is a reasonable choice resulting from cost and accuracy considerations. The grid points are concentrated in the injection location, the near outlet region and the near wall regions in order to maintain the accuracy of the turbulence model. The under-relaxation factors used to obtain a faster convergence are chosen as 0.5,0.5,0.4,0.4, and 0.7 for U,V,K,ε*, and ν_t*, respectively.

The iterations are terminated when the difference between the flow rates of inflow and outflow through the control volume is less than 10^{-6}.

It seems that there is no available data for direct comparison with the present results for the plain seal with injection. Therefore, for the verification purposes of the numerical method, the cases of internal flow different from the present one are chosen for comparisons. The present results are compared with those of Sharma et al.[10] and Kuzay et al.[11] for the angular momentum distribution for angular rotating cylinder. Figure 2 shows angular momentum profiles at Re ≈ 20000 and w = 6000 rpm. The current results agree well with the Kuzay's ones. However, there is some deviations between the present results and Sharma's. This may be attributed to the fact that Sharma et al. used mixing length theory as a turbulence model while standard k-ε model is employed in this study.

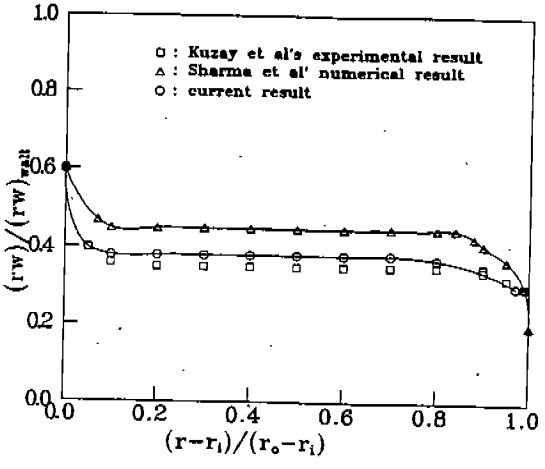

Fig.2 Comparisons of computed and measured angular momentum profiles

3. RESULTS AND DISCUSSION

Seals are usually used to reduce leakage in regions where the pressure gradient exists. Leakage rate is closely related to the pressure difference between the inlet and the outlet. When energy is actively dissipated due to the flow resistance, pressure difference between the inlet and the outlet increases and then leakage rate is diminished. Hence, seal performance is enhanced with the increase of the flow resistance.

The basic dimensions used in this study are listed in table 3, and the effects of the parameters on the leakage performance are investigated.

Table 3. Basic dimensions for the seal with injection

parameters	dimensions
inner radius (r_i)	22.5 mm
outer radius (r_o)	27.5 mm
axial length (L)	45.0 mm
clearance (c)	5 mm
injection location (b)	9.5 mm
injection width (d)	1 mm
injection angle (α)	90 degree

The velocity vector and streamline are presented in Fig.3 to show the flow pattern of the seal with injection. As shown in the figure, there exist the recirculation and reattachment due to the injection. One can also see that the streamline moves toward the stator by the rotor's centrifugal force.

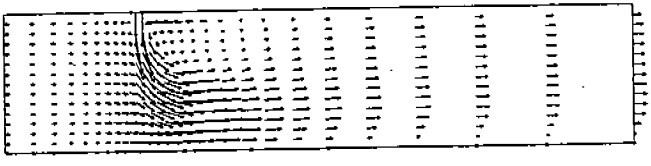

(a) velocity vector

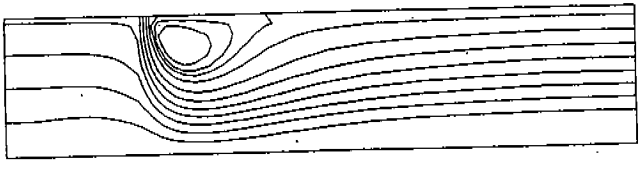

(b) streamline

Fig.3 Velocity vector and streamline profiles at Re=10000, w=10000rpm, $v_{in}=5u_{in}$

It is of special importance to investigate the effect of injection on the seal performance. The variation of pressure drop for both cases with and without injection is presented in Fig.4 as a function of rotation speed. Total inflow rate, Q, is assumed to be taken as a constant value of $Q = 8 \times 10^{-5}$ m^3/s. When there is a injection, the each amount of axial inflow flow rate and injection flow rate is taken as half of the total inflow rate, respectively. It is shown that the pressure drop for the case with injection, compared to the case without injection, increases more at all rotation speeds considered in this study. Hence, one can see that seal performance is enhanced with the addition of injection.

For a comparison of the leakage performance volumetric seal leakage amount is defined by

$$Q = C_L \cdot 2\pi r_i^2 \sqrt{2\Delta P/\rho}$$

where the leakage coefficient C_L is a dimensionless relative measure of the leakage to be expected from seals with the same radius.

Fig.5 shows the effects of the variation of injection flow rate on the leakage coefficient when the total flow rate is fixed. With the increase of the injection flow rate the leakage coefficient decreases,

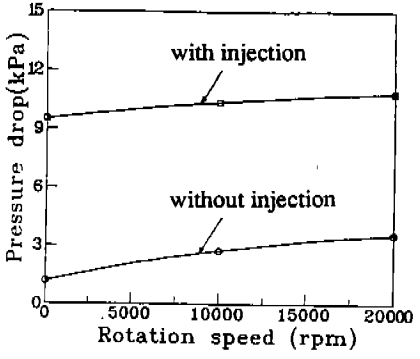

Fig.4 The injection effects on the pressure drop at the constant rotation speeds

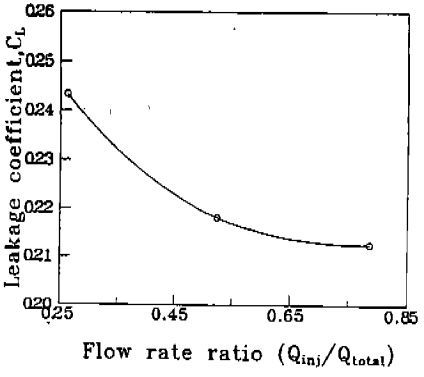

Fig.5 C_L versus injection flowrate ratio at w=10000rpm

and hence the leakage performance is improved. This phenomena can be explained by examining the distribution of the turbulence kinetic energy. As shown in Fig.6, the turbulence kinetic energy intensity has a large value at injection location, and is increased as the injection flow rate increases.

The increase of flow resistance due to the high turbulence kinetic energy intensity causes the increase of pressure drop, and hence the leakage performance is enhanced.

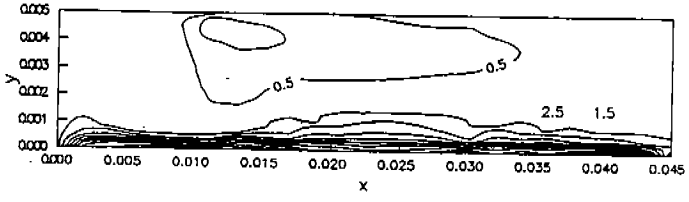

(a) flow rate ratio = 0.25

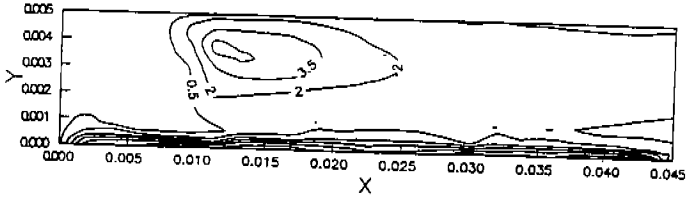

(b) flow rate ratio = 0.5

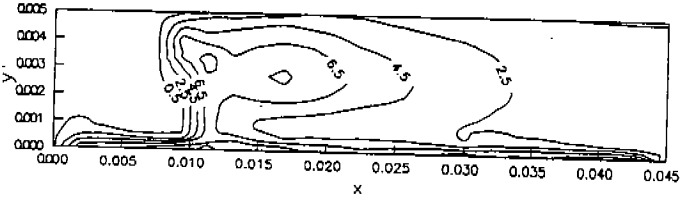

(c) flow rate ratio = 0.75

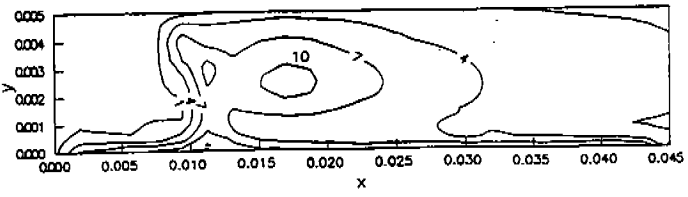

(d) flow rate ratio = 0.85

Fig.6 Iso-kinetic energy distribution diagram

Figure 7 shows the variation of the leakage coefficient as a function of the rotation speed. The leakage coefficient for the case without injection decreased with increased rotation speed because the pressure drop between the inlet and the outlet increases due to the high flow resistance resulting from the increases of the turbulence kinetic energy and dissipation as rotation speed increases. For the case with injection, the rotation speed has little effect on the leakage performance.

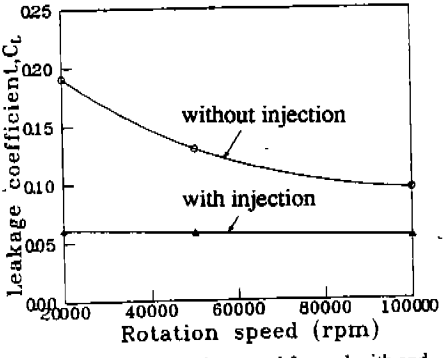

Fig.7 C_L versus rotation speed for seal with and without injection at Re=20000

Figure 8 illustrates the effect of injection angle on the leakage coefficient at the various values of injection flow rate. These profiles show that the leakage coefficient drops rapidly as the injection angle increases to 90 degree at which angle it has a minimum value, after this angle there is a smooth increase. This phenomenon is closely related to the shear layer between the recirculation zone and the streamlines resulting from injection. In a shear layer, energy is actively dissipated due to the high turbulent energy intensity. Enlargement of recirculation zone magnifies shear layer, and hence the energy dissipation rate is increased. Therefore, the leakage performance is enhanced with the increase of pressure drop. The size of the recirculation zone can be represented by the length from injection location to separation point. The reattachment lengths from the injection location are 1.63c, 1.74c, and 1.67c at injection angles of 45°, 90°, and 135°, respectively, where c represents the clearance. The size of recirculation zone and reattachment length depends mainly on the magnitude of the radial component of the injection velocity. The present numerical results show that the radial component of the injection velocity has a maximum value at the injection angle of 90 degree, at which angle the leakage coefficient has a minimum value due to the maximum pressure drop.

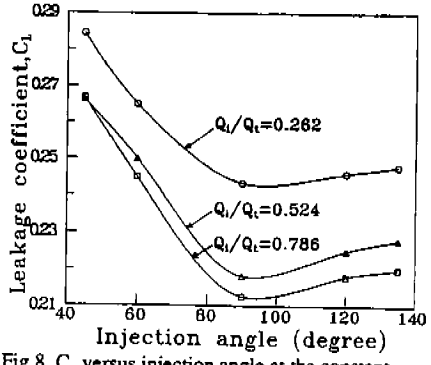

Fig.8 C_L versus injection angle at the constant total flow rate and w=20000rpm

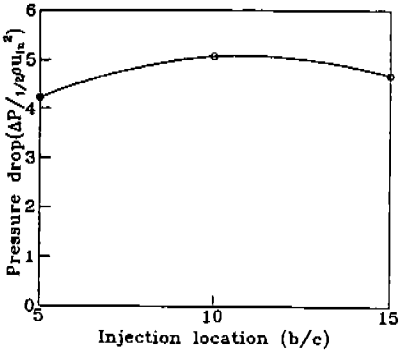

Fig.9 The effects of injection location on the dimensionless pressure drop at Re=10000, w=10000rpm

The variations of dimensionless pressure drop for the change of the axial injection location are presented in Fig.9. The profile shows that there is a smooth increase and decrease in pressure drop when the injection location is near the center of the seal. However, general trend indicates that the effect of the injection location on the pressure drop is not significant. It should also be pointed out that the present numerical approach cannot be applicable to the cases with the injection being applied near exit. In such cases there exists a circulation zone at the exit, and hence the reasonable results cannot be obtained due to the current method's limitations.

Figure 10 shows the dimensionless pressure drop as a function of the seal clearance ratio. It is shown that clearance ratio has a strong effect on the pressure drop, and that the pressure drop is increased rapidly with the decrease of the clearance ratio. However, the ranges of the clearance ratio should be restricted by considering the shaft eccentricity and friction generated between the rotor and stator. Therefore, the seal performance can be improved with the appropriate value within the proper ranges of the clearance ratio.

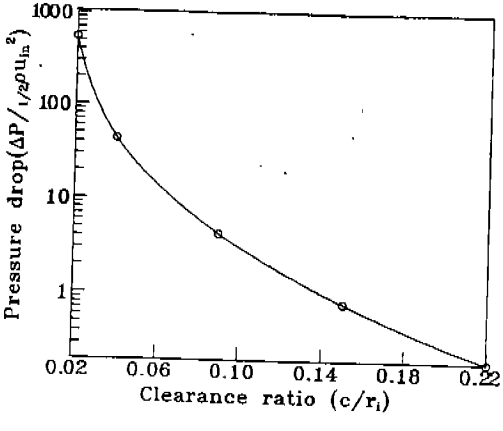

Fig.10 The effects of clearance ratio on the dimensionless pressure drop at Re=10000,w=10000rpm

4. CONCLUSIONS

Current work investigates the effects of various parameters on the characteristics of the flow field and leakage performance for the plain seal with injection. The conclusions can be summarized as follows :

1. The leakage performance is enhanced with injection.

2. With the increases of the injection flow rate and rotation speed, the leakage performance is improved.

3. The leakage coefficient has a minimum value at the injection angle of 90 degree.

4. Pressure drop has a maximum value when the injection is applied on the center of the seal, but there is no significant effect of the injection location on the pressure drop.

5. The clearance ratio has a significant effect on the pressure drop.

5. REFERENCES

1. C.C.Nelson, 1985, " Rotordynamic Coefficients for Compressible Flow in Taperd Annular Seals ", J. of Tribology, vol.107, July, pp.318-325.
2. R.Nordmann, F.J.Dietzen and H.P.Weizer, 1987, " Calculation of Rotordynamic Coefficients and Leakage for Annular Gas Seals by means of Finite Difference Techniques ", The 1987 ASME Design Technology Conference on Mechanical Vibration and Noise, Boston, Massachusetts, Setember 27-30, pp.351-357.
3. D.W.Childs and Chang-ho Kim, 1986, " Test Results for Round-Hole-Pattern Damper Seals : Optimum Configurations and Dimensions for Maximum Net Damping ", J.of Tribology,vol.108, October,pp.605-611.
4. H.Stoff, 1980, " Incompressible Flow in a Labyrinth Seal ", J. of Fluid Mech., vol.100, pp.817-829.
5. J.A.Demko, G.L.Morrison and D.L.Rhode, 1987, " Effects of Shaft Rotation on the Incompressible Flow in a Labyrinth Seal ", J. of Propulsion and Power, pp.508-520.
6. D.L.Rhode and S.R.Sobolik, 1986, " Simulation of Subsonic Flow Through a Generic Labyrinth Seal ", ASME, J.of Engineering for Gas Turbines and Power, vol.108, October, pp.674-680.
7. Y. Yamada, 1962, " Resistance of a Flow through an Annulus with an Inner Rotating Cylinder ", Bulletin of JSME, Vol.5, No.18, pp.302-310.
8. B.E.Lauder and D.B.Spalding, 1974, " The Numerical Computation of Turbulent Flows", Computer Methods in Applied Mechanics and Engineering, pp.269-289.
9. S.V. Patankar, 1980, Numerical Heat Transfer and Fluid Flow, McGraw-Hill, New York.
10. B.I.Sharma, B.E.Launder and C.J.Scott, 1976, " Computation of Annular, Turbulent Flow with Rotating Core Tube ", ASME J. of Fluid Engineering, December, pp.753-758.
11. T.M., Kuzay, and C.J., Scott, 1973, " Turbulent Heat and Momentum Transfer Studies in an Annulus with Rotating Inner Cylinder," University of Minnesota, Heat Transfer Laboratory, TR No.111, Dec..